WHITE PAPER

CURRENT RATING POWER CONNECTORS **USING VOLTAGE DROP CRITERIA**

BY
ROBERT D. MALUCCI & FRANK R. RUFFINO
MOLEX INC.
LISLE, ILLINOIS

molex

Current Rating Power Connectors Using Voltage Drop Criteria

Abstract	**3**
Introduction	**3**
Test Program	**3**
Test Results	**4**
Discussion	**6**
Data Analysis and Discussion	**7**
Conclusions	**10**
Acknowledgments	**10**
References	**10**

Author

ROBERT D. MALUCCI &
FRANK R. RUFFINO

ABSTRACT

A new approach in current rating power contacts using change in voltage drop is proposed. This method may replace the standard use of thermocouples to monitor temperature rise throughout an accelerated test series. Criterion was developed empirically from high current testing of tin plated power contacts. Data from accelerated aging tests followed by high current cycling tests is used to establish an empirical basis for change in voltage drop criteria. These results were analyzed using basic contact theory to relate loss of metallic contact to change in resistance criteria. The ultimate goal is to use change in contact resistance to evaluate the performance of power contacts.

Introduction

Last year at IICIT the present authors proposed that voltage drop change be used to evaluate high current performance of power contacts [1]. It was shown that when the voltage drop change of aged contacts crosses a threshold of 0.01 to 0.03 volts, that thermal instability ensues. This was demonstrated with plots of voltage drop change per cycle versus voltage drop change as shown in figure 1. While this type of data clearly shows a threshold that defines performance criteria, it does not provide a means to rate the contacts in question. Consequently, a method is needed that enables one to establish the current level at which a contact system can operate over it's expected life in the field. To this end the present paper addresses this issue by using voltage drop data from contacts subjected to accelerated aging tests. These data are analyzed statistically and used to correlate the results with subsequent failures observed during high current cycle tests. Consequently, the end of life voltage drop data is used to predict high current failures and provides a basis on which the power contacts can be current rated.

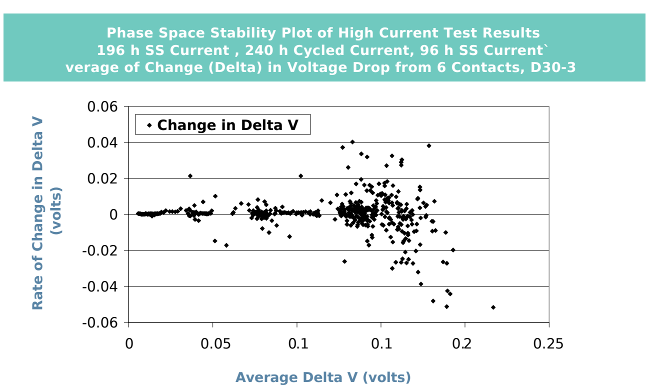

Figure 1: Stability Plot from Reference 1

Moreover, the test results for voltage drop change are related to physical changes that occur at the interface. Consequently, the change in voltage drop is related to loss of metallic contact at the interface. It will be seen for typical power contacts, that as the voltage drop change approaches 0.01 to 0.03 volts, metallic contact at the interface drops by more than an order of magnitude.

Consequently, the local current density increases by this factor causing excessive localized heating. These results are presented in the following sections.

Test Program

In addition to the data provided in reference [1], data were developed for the present work from other types of power contact systems. These contacts were tin plated square pin and socket types where each socket makes contact to two of the faces of the square pins. Consequently, this system provides two parallel paths through the pin and socket contact. In addition, the pin and sockets were housed in connectors containing 8 contacts. In these cases, samples were subjected to accelerated thermal aging tests during which the voltage drop of each contact was monitored periodically at various current levels. Unlike the data in reference [1], where six contacts from each connector were wired in series, the new data were taken on individual contacts. In addition, in the present case, the voltage and temperature were measured to demonstrate the level of correlation that exists between voltage drop change and temperature rise. In this test program, the samples were purposely aged beyond the end of life. Moreover, current levels were elevated to produce voltage drop changes that rose to the threshold levels of the 0.01 to 0.03 Volts. Generally, this required using current levels above the rated current for these types of power contacts. Subsequently, the samples were subjected to high current cycle tests using the currents that produced the 0.01 to 0.03 voltage drop change.

TEST RESULTS

Figures 2a and 2b provide typical change in voltage drop data for two cases subjected to thermal aging tests. The data are provided as distributions of voltage drop change at three stages of the thermal aging test. These cases were experimental samples constructed with high conductivity base metals.

Voltage Drop Change Distribution Through Thermal Age Tests
Case 1, Tin Plated Pin and Sockets, 17 Amps

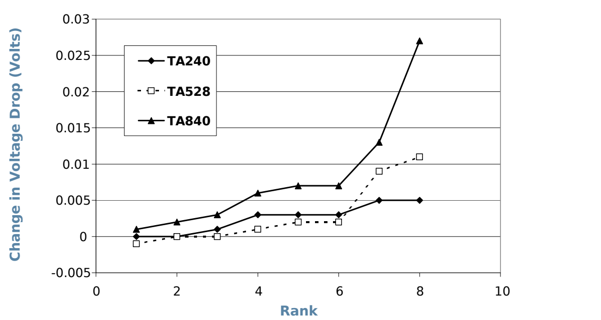

Figure 2a: Case 1 Distribution

Voltage Drop Change Distribution after Thermal Aging
Case 2, Tin Plated Pin and Sockets, 20 Amps,

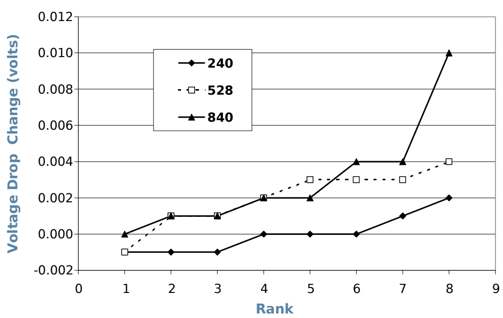

Figure 2b: Case 2 Distribution

As shown, the ranked data of voltage drop change at each phase on the thermal aging test is provided. The current levels used in these cases produced end of life (840 hrs at 105 °C) voltage drop changes near the 0.01 to 0.03 Volt levels. Subsequently, these current levels were used to conduct the high current cycling tests. Generally, as the samples aged, the voltage drop change levels increased as seen in these plots. The data in figure 2a shows samples that exhibit values of change in voltage drop approaching 0.03 Volts at17 Amperes (case 1). The data in figure 2b shows samples approaching 0.01 Volts at 20 Amperes (case 2). It should be noted that these two cases represent different base metals and therefore aged differently.

Moreover, these cases approached the range of voltage drop changes that define temperature instability. This can be seen in figures 3a and 3b where stability plots from subsequent high current cycle tests (similar to the plot in figure 1) are provided for the two cases shown in figures 2a and 2b.

Stability Plot of Change in Voltage Drop
Case 1, Tin Plated Pin and Socket, 8 Contacts
High Current Results at 17 Amperes After Thermal Aging

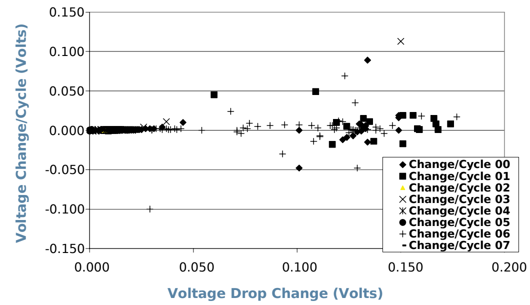

Figure 3a: Stability Plot of Case 1

Stability Plot of Change in Voltage Drop
Case 2, Tin Plated Pin and Socket, 8 Contacts
High Current Results at 20 Amperes After Thermal Aging

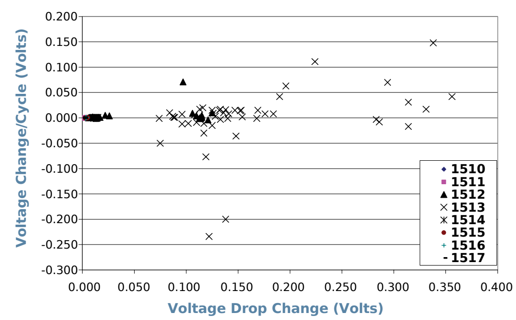

Figure 3b: Stability Plot of Case 2

It should be noted that the high current cycle tests employed a test-to-failure strategy to verify the impact of crossing the stability threshold. Consequently these tests validate the concept that for aging contacts, performance can be judged using change in voltage. In these cases, unlike the case in figure 1, the individual contacts were monitored for voltage drop and temperature. The plots in figures 3a and 3b clearly show that instability occurs as the voltage drop change approaches and surpasses the threshold level of 0.03 Volts. A closer look at the high current cycle data for case 1 is shown in figure 3c where one can clearly see the transition to instability for the four samples that failed.

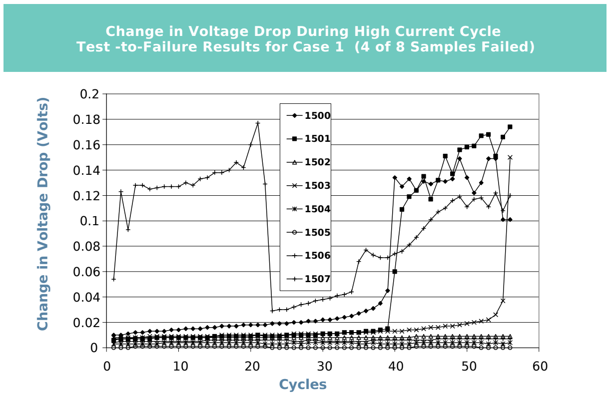

Figure 3c: Case 1 Current Cycle Results

Clearly, as the samples degrade to levels above 0.01 to 0.03 Volts change they rapidly go into thermal runaway. In these cases the failed samples rose to the melting voltage of tin (0.143 Volts). It should be noted that the high current tests were conducted at current levels about twice the rated current for this type of design, so it's not surprising that marginal samples failed quickly in the high current cycle phase of the test. Moreover, as one looks closer at the initial values of voltage change (cycle 1) it is seen that samples that approached or exhibited values around 0.01 Volts subsequently continued to degrade until they crossed the threshold of 0.01 to 0.03 Volts change. These samples exhibited thermal runaway as they rose to the melting voltage of tin. This is an important point and will be discussed in the next section.

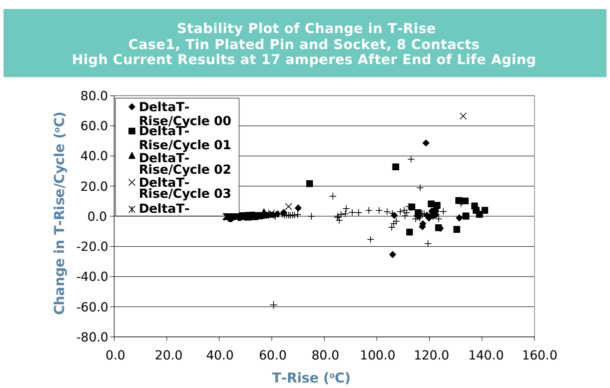

Figure 4a: Stability Plot of Case 1

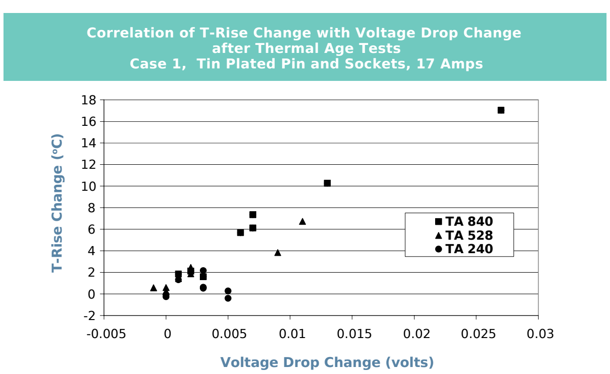

Figure 4b: Correlation of T and V Case 1

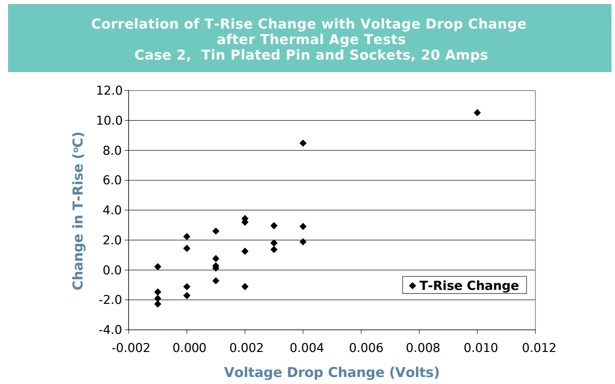

Figure 4c: Correlation of T and V Case 2

In addition, figure 4a shows a plot of the change in temperature-rise for the samples in figure 3a. It is obvious that the change in temperature-rise closely follows the same patterns seen in the change in voltage drop plots. It is apparent that a correlation exists between voltage drop change and change in temperature-rise. Figures 4b and 4c show plots of change in voltage drop versus change in temperature-rise as seen during the thermal age test series. These results show change in temperature-rise data, while exhibiting some scatter, correlate well with change in voltage drop throughout the entire test series. This was observed in all cases studied.

One can summarize these results by saying that they support the following

1. There's a strong correlation between monitoring voltage drop and temperature
2. On an individual contact basis, a threshold for thermal instability appears to occur as the change in voltage drop approaches the range 0.01 to 0.03 Volts.
3. It is believed the voltage drop results from aging tests can be used to predict thermal instability

The last statement is based on the fact that both samples exhibited a distribution of voltage drop changes that approached the lower and upper end respectively of the stability threshold (at the end of the thermal aging tests). Consequently, one can say that there's a chance of thermal instability in these samples if subjected to high currents. This is exactly what happened as seen in figures 3a, 3b and 3c. However, it is also seen in these plots that the sample at the upper end of the threshold region (case 1), produced twice as many failures in the high current cycling phase of the test. These results indicate that one needs to take a closer look at how voltage drop change data should be interpreted. This requires a statistical analysis of the data to provide a method of predicting reliability at a given current level. Moreover, as discussed in the next section, this analysis considers the physical changes that occur at the interface as aging progresses.

Discussion

In an effort to understand the present test results, an analysis of the contact design was undertaken. Moreover, a statistical analysis of the voltage drop data was conducted to provide a statistical basis for the evaluation of high current performance. First it is recognized that the pin and socket contact produces two contacts in parallel and therefore the current takes two paths through the socket. In addition, the current will split according to the resistance in each path. Since contacts vary statistically, in general, even though the samples were subjected to the same level of aging, individual contacts from a distribution do not exhibit the same change in resistance. Consequently, during aging, one would expect the current to differ through each path. However, both paths will exhibit the same voltage drop as they are electrically in parallel.

Pin an Socket Equivalent Circuit

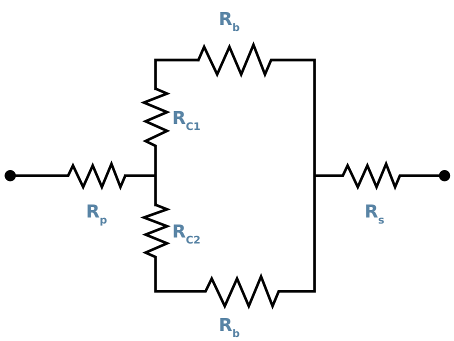

Figure 5: Circuit Diagram

Figure 5 shows a schematic of the equivalent circuit of the pin and socket design. From this diagram one can calculate the effective contact resistance in terms of the bulk resistance (R_b) and contact resistance (R_c) in each path. In addition, there are also bulk resistances associated with the contact members external to the parallel paths. These are denoted as R_p and R_s for the pin and socket respectively. With these definitions, the overall pin and socket resistance is given as,

$$R_{eff} = R_p+R_s+(R_b+R_{c1})(R_b+R_{c2})/\ 2R_b+R_{c1}+R_{c2} \quad (1)$$

Where the subscripts 1 and 2 refer to the two parallel paths through the socket as shown in figure 5.

As the contact ages, equation 1 can be used to calculate the change in resistance. Assuming the bulk resistance components remain constant during aging and initially $R_{c1} \approx R_{c2} = R_c$, after some algebra from equation 1, one gets,

$$\Delta R = (R_o/2)\{(\Delta R_{c1}+\Delta R_{c2})/2\ R_o + (\Delta R_{c1}\Delta R_{c2})/\ /Ro^2\}/\{1+(\Delta R_{c1}+\Delta R_{c2})/2\ R_o\} \quad (2)$$

Where $R_o = R_b + R_c$ is the initial resistance of each of the parallel paths through the socket. Equation 2 is useful in analyzing the changes that occur at the contact interfaces as the overall resistance is observed to change. The change in voltage drop (ΔV) that's observed is the current (I) times the change in resistance (ΔR) given by equation 2. Thus,

$$\Delta V = I\ \Delta R \quad (3)$$

Consequently, using equations 2 and 3 one can relate the change in voltage drop to the change in resistance at the two contact interfaces. However, since the contact resistance in each parallel path differs as the contact ages, one can only approximate the changes that occur in each case. This is done by evaluating several casesThis is done by evaluating several cases that cover the range of differences in Rc that can occur in each path. To do this the expression ΔRc1= βΔRc2 is substituted in equation 2 to provide an expression where different values of β are chosen to calculate ΔRc1and ΔRc2 as a function of ΔV. In effect, using the factor β, the change in resistance at each interface can be calculated by inverting equation 2 as follows.

$$\Delta R_{c2} = (1+\beta)(1\text{-}K)/2\beta + \{(1+\beta)^2(1\text{-}K)2 + 4\beta K\}^{1/2}\ /2\beta \quad (4a)$$

$$\Delta R_{c1} = \beta \Delta R_{c2} \quad (4b)$$

Where K = 2ΔV/I R_o. Moreover, $\Delta R_{c1}$and ΔR_{c2} can be used to estimate the loss of metallic contact at each interface using the well-known Holm [2] model for multi-point contacts. The expression for a circular contact spot of apparent diameter, D, is given as,

$$R_c = \rho_b/D + \rho_p/nd \quad (4c)$$

Where ρ_b and ρ_p are the resistivities of the contact base metal and plating respectively. In addition, n is the number of real contact spots and d the average size of the spots. Since the real contact area is the sum of the multi-point contact areas, equation 4c can be used to relate real contact area to contact resistance. If we assume the first term in equation 4c remains constant, as the contact ages the change in resistance is given as,

$$\Delta R_c = \rho_p\ /nd - \rho_p\ /n_i d_i \quad (5)$$

Where the subscript, i, refers to the initial contact before aging. The analysis can be simplified by assuming the contact spots are circular and similar in size. Consequently, the metallic contact area can be estimated as $A_m \approx \pi n d^2/_4$. Using this expression in 5 and performing some algebra, expressions for the following two cases were derived.

$$\text{For } d_i = d\text{: } A_1/A_o = 1/(1 + \Delta R_c/R_{ms})^1 \quad (6a)$$

$$\text{For } n_i = n\text{: } A_2/A_o = 1/(1 + \Delta R_c/R_{ms})^2 \quad (6b)$$

Where the substitution of $R_{ms} = \rho/n_i d_i$ was made. The first case represents the loss of metallic contact by reduction of the number of spots with the spot size remaining constant. The second case is for loss of metallic contact by reduction of spot size for a fixed number of spots. Since in the real world one would expect metallic contact loss to occur by both loss of number and size, the average of 6a and 6b were used to estimate the remaining contact area.

Equations 6a and 6b were used to estimate the total remaining metallic contact from both contact interfaces after a change in resistance occurs in each. Figure 6 provides the results for a wide range of values for ρ that cover the possible cases that may occur in real situations. Moreover, in this case, the values for R_{ms} and R_o were estimated to be 0.3×10^{-3} and 0.8×10^{-3} Ohms respectively and the current level was 17 Amperes. Consequently this plot represents the case shown in figure 3a. As one can see, this simplified analysis indicates that at voltage drop changes from 0.01 to 0.03 Volts, the real metallic contact area drops below 10% of the initial value. This represents more than an order of magnitude change in total metallic contact for this type of design. Consequently, the range of about 0.01 to 0.03 volts defines a transition for metallic contact to fall below 10% of the original contact (and thereby producing excessive localized heating in the contact interface region). Based on this discussion, one might expect excessive heating and instability to occur at high currents as the voltage drop change approaches these levels of change.

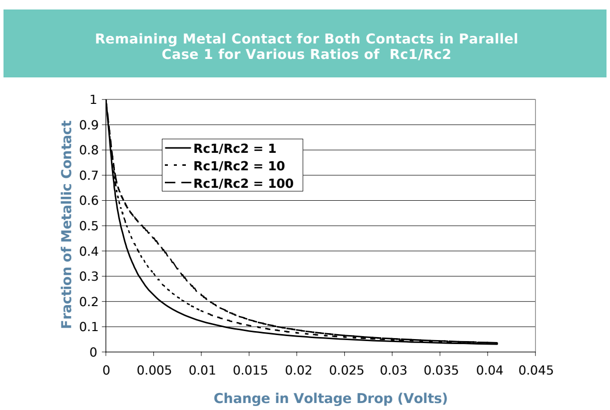

Figure 6: Remaining Metal Contact

Data Analysis and Discussion

As seen in the physical model, when the change in voltage drop exceeds the 0.03 Volt level, the remaining metallic contact area was estimated to have changed by more than an order of magnitude. Consequently, one expects excessive localized heating as shown in the data plots. However, all of these data were obtained at current levels significantly above the standard current rating for the terminal. This was done in an effort to create failures in the high current test phase. In the standard design, the rated current is 7 to 9 Amperes, whereas the high current cycle tests in the present experiments were conducted at 17 and 20 Amperes respectively. In order to develop a methodology to rate the contacts using change in voltage drop, one needs to provide a way of statistically analyzing the voltage drop results. For example, in looking at the data in figures 2a and 2b, one sees a distribution of values for change in voltage drop at the end of the thermal aging test. This data exhibits values that range from below the stability threshold (0.01 Volts) to the top end of the threshold (0.03 Volts). Moreover, some of the cases above the 0.01 Volt level did not subsequently fail, while others that were below this level did. In other words, one cannot in general predict the outcome of an individual contact in subsequent high current confirmation tests. However, it is believed this problem is statistical in nature. What one needs to do is predict from the distribution what the probability is to exceed the threshold and compare this to the actual results on a statistical basis.

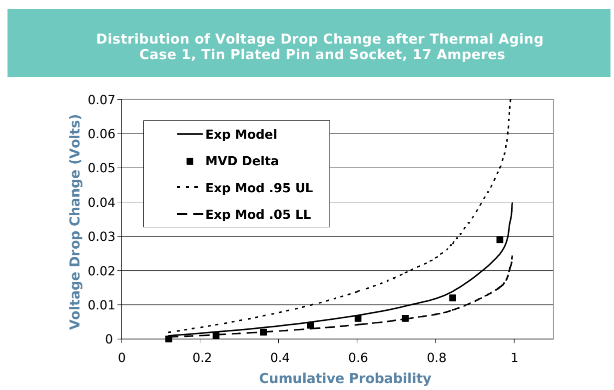

Figure 7a: Case 1 Voltage Change Distribution

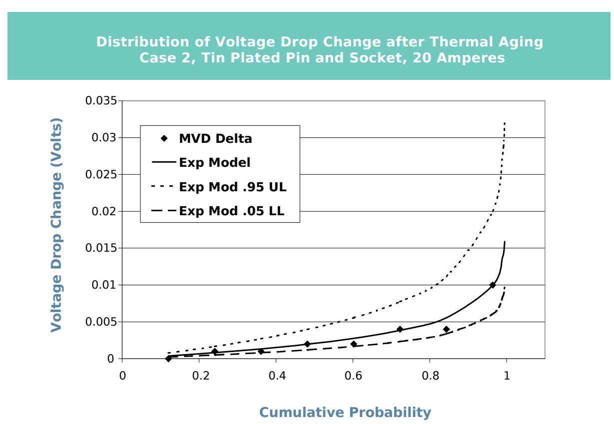

Figure 7b: Case 2 Voltage Change Distribution

To begin, a statistical distribution was fit to the end-of-life change in voltage data, as shown in figures 7a and 7b. Also shown in these plots are the upper 95% and lower 5% curves for these cases. Subsequently, these distributions, while recognized as limited by the sample size, were used to predict statistically the chance to exceed the threshold. The statistical model used was a one parameter exponential distribution that enabled calculating the probability of exceeding a specific voltage drop change at a given confidence level. This model is defined as follows.

$$P(\Delta V_c > \Delta V_t) = e^{-\Delta V_t/\Lambda} \qquad (7)$$

Where P is the probability that ΔV_c , the change in contact voltage, exceeds ΔV_t ,the threshold voltage. Λ is the average (or expectation value) of the change in voltage drop for the end-of-life distribution. It should be noted that all the fits used in this analysis were validated using Bartlett's test [3] at the 5% and 95% significance levels. Moreover, this model was used to estimate statistically the threshold voltage change that produced the failures observed in the high current tests. The latter was accomplished by using the voltage drop change distribution that was observed at the onset of failure during the high current test. This was done at three stages of the current cycle test that clearly showed the progression of failures (see figure 3c). In these cases failure was defined when a sample showed erratic behavior. For example, at the 34-cycle point, one sample showed a large jump at the next cycle. The additional cases were at the 39 and 55 cycle points where 2 and 1 additional failures occurred respectively. Λ was calculated from the distribution of values at each of these points by taking the average. Subsequently ΔV_t was calculated using equation 7. The results are summarized in table 1 below.

Table 1

CYCLE	$P(\Delta V_C > \Delta V_T)$	Λ(V)	ΔV_t(V)
34	1/8	0.014	0.029
39	3/8	0.019	0.019
55	4/8	0.053	0.037

From these results the average ΔV_t was determined to be 0.028 Volts. As one can see this statistical result is in agreement with the data provided in figures 3a and 3b and provides confidence that this threshold value is useful in calculating the probability of failure from equation 7. One should note that the value of Λ is determined from the distribution of change in voltage drop. Consequently, if the end of-life Λ is determined from aging tests then this model may be used to calculate the end-of-life probability of failure. As an example of how this method is used, the value for ΔV_t of 0.028 Volts defines a predictive threshold for high current cycle failures at 17 Amperes in case 1. That means that this value in voltage drop change can be used in equation 7 to calculate the expected probability of failure in the high current tests. It is interesting to compare this value of voltage drop change to the chart in figure 6. As seen, a 0.028 voltage change corresponds to an estimated loss of metallic contact of more than an order of magnitude. It should be noted that the current used in the high current tests is the same current that was used to produce the end-of-life voltage drop change distribution (figures 7a and 7b). Moreover, the value for Λ is obtained from the end-of-life data set for change in voltage drop. In the cases studied in this work, it was found that the nominal values for end-of-life average voltage change, Λ, were 0.008 and 0.0036 Volts for the two cases in figures 7a and 7b respectively. Consequently, from equation 7 one can estimate the probability to exceed the .028 Volt level. For case 1, the upper 95% and lower 5% levels were calculated as 0.175 and as 0.003 respectively. With these probabilities, one sees that for a sample of 8, it is expected that nominally from 1.4 to 0 failures would be observed in the beginning of the high current tests. As seen in figure 3c, this prediction is in agreement with the one failure that occurred at the onset of the high current test.

In summarizing this discussion, it should be noted that the two factors ΔV_t and Λ, and the end-of-life statistical failure criteria, need to be determined in using this approach. For example, in case 1, Λ is plotted as a function of current for the present data set in figure 8.

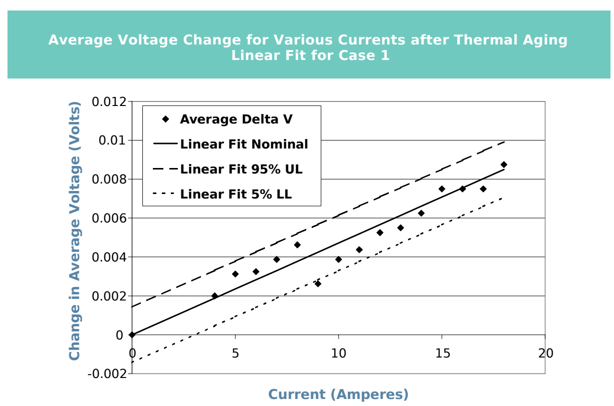

Figure 8: Case 1 Average V vs I

As one can see, even though the data exhibit significant scatter, Λ increases as the current increases as expected. The solid curve represents a linear fit and may be used to model Λ as a function of current for that case. However, even with Λ known, one still needs to determine ΔV_t for the current level in question. The latter may differ from ΔV_t at other currents as the bulk temperature rise differs.

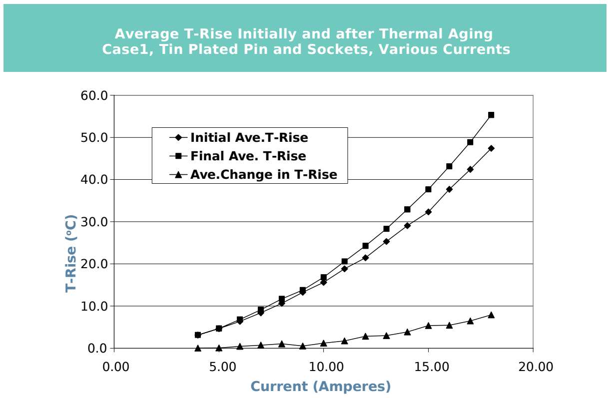

Figure 9: Case 1 Average Temperature Rise

Figure 9 provides the temperature rise results for case 1. Shown in the plot is the initial and post thermal age temperature rise as a function of current. In case 1, 17 Amperes were used to produce high current failures in the current cycling tests as shown in figure 3c. Two factors are revealed in this plot. First the average bulk temperature rise at 17 Amperes is more than 3 times the rated current for this design (9Amperes). Second, the change in temperature rise due to aging approaches 10 °C at 17 Ampere (as opposed to less than 1 °C at 9 Amperes). Consequently, elevated currents impact both the bulk temperature rise and its change due to aging. The impact these factors have on end of life performance needs to be determined before one can confidently de-rate a contact system using elevated current tests. This was not done in the present experiments and needs to be addressed in future work. In order to do this, one needs to determine how elevated bulk temperature accelerates aging in current cycling tests and what impact local current density has on the contact interface degradation. It's likely these two factors are related. For example, as the contact ages, the current density increases as metallic contact decreases. Moreover, as the current is increased, in addition to a bulk temperature increase, the current density across the contact increases as well.

While current density effects were not investigated directly, the impact can be estimated on the basis of physical considerations. For example, in the case of 17 Amperes a value of 0.028 Volts change defines the threshold ΔVt for this current level. As discussed above, the loss of metallic contact was estimated using equations 6a and 6b in conjunction with the present design characteristics as shown in figure 6. Since the current density J equals I/A one can use equations 6a and 6b as follows.

$$J = I/\{A_o/(1 + \Delta R_c/R_{ms})^n\} \quad (8)$$

Where the two cases for n = 1, 2 will be considered. If initially the effects of bulk temperature are neglected. One can proceed by assuming the same current density across the contact in each case will produce a similar number of failures at that current. Consequently, equation 8 can be used by equating the threshold current density of the high current case to the current density at a lower current. Subsequently, one can use the observed high current threshold value to calculate the threshold at a lower current. In following this logic and after some algebra, the following result was obtained.

$$\Delta V_t(9)/\Delta V_t(17) = 1.15 \quad (9)$$

This result shows, that from a current density point of view, the voltage change threshold doesn't appear to be too much different at about half current level (about 15% in this case). Consequently, with this result, aside from the fact that elevated temperature swings are known to accelerate degradation [4], one is left with pursuing the impact of elevated bulk temperature on threshold voltage change. This remains to be studied in a future program. To complete this discussion, data taken at 9 Amperes, as shown in figure 10, was used in conjunction with the result in equation 9 to estimate the upper limit on failure rate at this current.

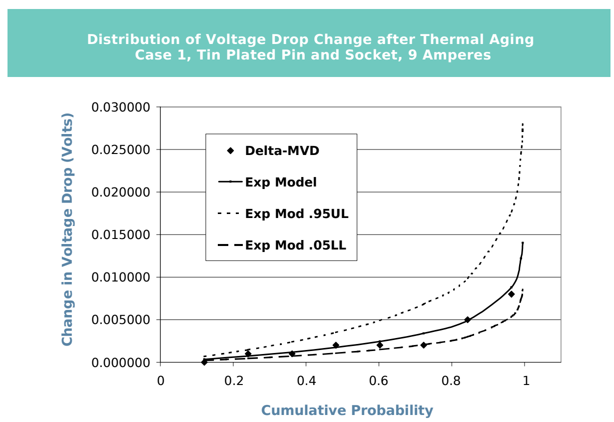

Figure 10: Case 1 Distribution at 9 Amperes

This involved using Λ from the distribution in figure 10. For the 9 Ampere case $\Delta V_t(9)$ was found to be 0.0322 and from figure 8, $\Lambda = 0.004$, the upper 95% result was obtained as follows.

$$P\,(\Delta V_c > \Delta V_t(9)) < e^{-\Delta V_t/\Lambda} < 0.018$$

This result shows that at 9 Amperes the end-of-life expected failure rate falls by about an order of magnitude below the rate at 17 Amperes (which is 0.175). However, one would expect the actual probability to be even less, as the bulk temperature rise is three times less than the 17 Amperes case. Consequently, the aging factor associated with the temperature swing would be less in the 9-Ampere current cycling test.

These results while not complete, are very encouraging and support the strategy of using change in voltage drop statistically to current rate a contact system. What needs to be done in applying this method is to find the current level where statistically the samples meet specific reliability requirements. Subsequently, a confirmation test at this current should be conducted. In other words, one runs aging tests and measures the voltage drop change distribution at various currents. Subsequently, the data can be fit to a distribution, such as the exponential type, to predict the probability of exceeding the stability threshold at a specific confidence level. The current at which the samples meet the statistical requirements would then be used to conduct high current confirmation tests such as current cycling.

Conclusions

It was seen that a stability threshold exists in change in voltage drop that can be used to define failure criteria for power contacts. In addition, it was shown that this data requires a statistical treatment to interpret the results of a given contact system. Subsequently, the statistical analysis enables one to define the risk of using the contacts at a given current level. This approach correlated very well with the test cases presented in this analysis. However, while this approach clearly established a method of predicting the chance of failure at the current levels tested in this study, it did not provide confirmation tests on the proposed current levels that are safe over the life of the contact. As discussed above this requires determining acceleration factors due to elevated bulk temperature and elevated current density across the interface. However, as shown in the example above, the contacts studied in this work are rated at levels that are consistent with the present results. Consequently, it is recommended that this approach be seriously pursued as a methodology in rating power contacts. To this end, it is recommended that evaluation of high current confirmation tests be conducted to establish the validity of this method.

Acknowledgments

The authors would like to thank Bob Smid, from Molex product reliability laboratory, for collecting and helping format the voltage drop and temperature rise data provided in this analysis.

References

[1] R.D. Malucci and F.R. Ruffino, "Voltage Drop Stability as a Method of Rating Power Contacts", IICIT Proceedings, 2003

[2] Holm, "Electric Contacts" , Springer-Verlag, 1967, pp. 21

[3] K.C. Kapur and L.R. Lamberson, "Reliability in Engineering Design", Wiley, 1977, pp239

[4] R.D. Malucci " Fretting Corrosion Degradation, Threshold Behavior and Contact Instability", Proceedings of the Forty-Ninth IEEE Holm Conference on Electrical Contacts, 2003, p.2

Originally published in 2004/2005.

Order No. 987652-4993 USA/0K/GF/2022.03